

PEDRO M. RAMOS^{1,2}, TOMÁŠ RADIL¹, A. CRUZ SERRA^{1,2}

¹Instituto de Telecomunicações, Lisbon,

² DEEC, Instituto Superior Técnico, Technical University of Lisbon
Portugal

e-mail: pedro.ramos@lx.it.pt, tomas.radil@lx.it.pt, acserra@ist.utl.pt

FOUR-PARAMETER SINE-FITTING ALGORITHM FOR DETECTION AND CLASSIFICATION OF TRANSIENTS AND WAVEFORM DISTORTIONS

This paper describes a new method for detection of some power quality (PQ) disturbances, namely transients and waveform distortions. The proposed algorithm is based on a modified version of the four-parameter sine-fitting algorithm. The sine-fitting algorithm is used to estimate the parameters of the power system's voltage signal's fundamental and to extract the transient component of the voltage. The performance of the proposed method is compared with previously developed algorithm and with two commercial PQ analyzers.

Keywords: power quality, sine-fitting algorithms, mathematical morphology, transients, waveform distortions.

1. INTRODUCTION

Transients and waveform distortions are one of the most common types of power quality disturbances. Although they do not represent such an inconvenience as interruptions and sags or the danger of swells, they can represent a serious problem as the magnitude during the transients can reach up to 4 pu (pu = per unit; relative voltage scale normalized using the power system's nominal voltage RMS value) and the high frequency components of transients and waveform distortions can affect the operation of equipment connected to the power network (*e.g.*, motors).

Methods for detection of transients and waveform distortions use algorithms to separate the fundamental of the voltage signal and the transient component that contains the information about the disturbance. The traditionally used methods include: calculating the cycle-by-cycle difference (comparing a cycle of the voltage signal with a previous cycle); comparing the measured voltage waveform with an average fundamental waveform and using high-pass or notch filters [1]. Algorithms based on the wavelet transform are also frequently used for transient detection [2].

¹ Received: November 4, 2008. Revised: November 25, 2008.

In this paper, a method based on a modified four-parameter sine-fitting algorithm is presented. The performance of the proposed method is compared with the solution earlier published by the authors based on a digital high-pass filter [3] and with two commercial power quality analyzers.

2. DETECTION AND CLASSIFICATION OF TRANSIENTS AND WAVEFORM DISTORTION

The proposed algorithm uses sine-fitting algorithm and a mathematical morphology operation called closing to extract, detect and classify disturbances present in the voltage signal. The block diagram of the algorithm is shown in Fig. 1.

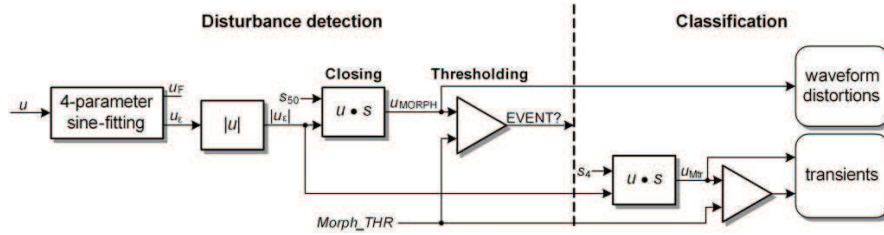


Fig. 1. Block diagram of the detection and classification method.

First, the algorithm uses the four-parameter sine-fitting to separate the voltage's fundamental u_F and the transient component containing potential disturbance u_ε . To simplify the detection process, the signal u_ε is processed using the mathematical morphology operation closing. After thresholding, if there is an event in the data segment being processed, the algorithm proceeds to the classification stage where the type of disturbance (transient or waveform distortion) together with the disturbance's parameters (magnitude, duration) are determined.

The main steps of the proposed algorithm (*i.e.*, sine-fitting, closing operation and classification) are described in the following subsections.

2.1. Extraction of the disturbance using four-parameter sine-fitting algorithm

Any component of the measured voltage other than the fundamental component represents a potential disturbance and has to be analyzed. Therefore an algorithm for detection and classification of power quality disturbances has to separate the fundamental component u_F and the component containing possible disturbances u_ε

$$u = u_F + u_\varepsilon. \quad (1)$$

The algorithm for PQ disturbance's detection described in this paper is based on sine-fitting algorithm. The sine-fitting algorithm estimates the parameters (amplitude, phase, frequency and DC component) of the fundamental u_F . The signal u_ε is then calculated as the difference between the estimated fundamental and the actual measured signal.

The proposed algorithm uses the modified four parameter sine-fitting algorithm. This modified algorithm improves the convergence of the known four-parameter algorithm [4]. The four-parameter sine-fitting algorithm estimates the fundamental's in-phase (A) and quadrature (B) components, the DC component (C) and signal frequency ω

$$u_F = A \cos(\omega t) + B \sin(\omega t) + C. \quad (2)$$

The initial frequency estimate $\omega^{(0)}$ is obtained using the interpolated DFT algorithm [5]. The initial estimate of the rest of the parameters (A , B , C) is obtained using the three-parameter sine-fitting algorithm [4].

After calculating the initial estimates, the algorithm proceeds to the iterative part of the four-parameter sine-fitting. First, the reconstructed estimate $\hat{u}_F^{(0)}$ of the signal u_F is determined using (2). In each iteration step, the algorithm builds a matrix $\mathbf{D}^{(i)}$

$$\mathbf{D}^{(i)} = \begin{bmatrix} \cos(\hat{\omega}^{(i-1)} t_0) & \sin(\hat{\omega}^{(i-1)} t_0) & 1 & -\hat{A}^{(i-1)} t_0 \sin(\hat{\omega}^{(i-1)} t_0) + \hat{B}^{(i-1)} t_0 \cos(\hat{\omega}^{(i-1)} t_0) \\ \cos(\hat{\omega}^{(i-1)} t_1) & \sin(\hat{\omega}^{(i-1)} t_1) & 1 & -\hat{A}^{(i-1)} t_1 \sin(\hat{\omega}^{(i-1)} t_1) + \hat{B}^{(i-1)} t_1 \cos(\hat{\omega}^{(i-1)} t_1) \\ \vdots & \vdots & \vdots & \vdots \\ \cos(\hat{\omega}^{(i-1)} t_{M-1}) & \sin(\hat{\omega}^{(i-1)} t_{M-1}) & 1 & -\hat{A}^{(i-1)} t_{M-1} \sin(\hat{\omega}^{(i-1)} t_{M-1}) + \hat{B}^{(i-1)} t_{M-1} \cos(\hat{\omega}^{(i-1)} t_{M-1}) \end{bmatrix} \quad (3)$$

and uses this matrix to calculate the vector $\Delta \hat{x}^{(i)}$

$$\Delta \hat{x}^{(i)} = \begin{bmatrix} \Delta \hat{A}^{(i)} & \Delta \hat{B}^{(i)} & \Delta \hat{C}^{(i)} & \Delta \hat{\omega}^{(i)} \end{bmatrix}^T = (\mathbf{D}^T \mathbf{D})^{-1} \mathbf{D}^T (u - \hat{u}_F^{(i-1)}). \quad (4)$$

of changes of the parameters being estimated. M is the number of samples and t_i are timestamps of individual samples.

The vector $\Delta \hat{x}^{(i)}$ is then used to update the vector of estimated parameters $\hat{x}^{(i)}$

$$\hat{x}^{(i)} = \begin{bmatrix} \hat{A}^{(i)} & \hat{B}^{(i)} & \hat{C}^{(i)} & \hat{\omega}^{(i)} \end{bmatrix}^T = \hat{x}^{(i-1)} + \Delta \hat{x}^{(i)}. \quad (5)$$

Using the newly estimated parameters, $\hat{u}_F^{(i)}$ is determined and the root-mean-square error of estimation is obtained using

$$\varepsilon_{RMS}^{(i)} = \sqrt{\frac{1}{M} \sum_{m=0}^{M-1} (u_m - \hat{u}_{F,m}^{(i)})^2}. \quad (6)$$

If the change of the RMS error since the last iteration step is smaller than a certain level (experimentally set to 10^{-2}) or if the maximum number of allowed iterations (set to 50) is exceeded, the algorithm is stopped and u_ε is determined from

$$u_\varepsilon = u - \hat{u}_F. \quad (7)$$

2.2. Processing using morphology operation closing and disturbance detection

The signal u_ε can be already used for disturbance detection using thresholding. However, since many of the disturbances that occur in power systems have an oscillatory character (*e.g.*, oscillatory transients caused by capacitor switching [1]) there are often multiple crossings of the threshold level that belong to the same disturbance. To simplify the detection and classification task, the signal is pre-processed before thresholding. First, the absolute value of the signal u_ε is calculated. The mathematical morphology operation closing [3][6] is then applied to the signal $|u_\varepsilon|$. Mathematical morphology operations are frequently used in image processing to process signals based on their shape. These operations apply to the processed signal a function called structuring element to highlight certain signal's features. The proposed method uses the closing operation to obtain the envelope of the signal $|u_\varepsilon|$ thus removing the multiple crossings of the threshold level that belong to one disturbance

$$u_{MORPH} = |u_\varepsilon| \bullet s_{50}. \quad (8)$$

where s_{50} is the structuring element. The structuring element s_{50} is a binary signal with the length of 50 ms (2 500 samples at sampling rate 50 kS/s).

The closing operation is composed of two other morphology operations: dilation \oplus and erosion \ominus that use the same structuring element s

$$u \bullet s = (u \oplus s) \ominus s. \quad (9)$$

A sample of the output signal of any mathematical morphology operation is obtained using the corresponding input sample and the samples in its neighbourhood. The size and shape of the neighbourhood are defined by the employed structuring element. In case of mathematical morphology, the structuring element is a binary signal containing a combination of zeros and ones: one indicates that the input sample at the corresponding position should be included in the calculation; zero means it will be omitted. The whole output sample is obtained by moving the structuring element along the input signal and at each position performing the respective morphology calculations using the input samples that lay on the positions where the structuring element is equal to one. In case of dilation and erosion the calculations are

$$(u \oplus s)[n] = \max \{u[n - m]\} \quad \forall s[m] \neq 0, m \in S, n - m \in U, \quad (10)$$

and

$$(u \ominus s)[n] = \min \{u[n + m]\} \quad \forall s[m] \neq 0, m \in S, n + m \in U, \quad (11)$$

respectively, where

$$S = \begin{cases} \{-(N_S - 1)/2, \dots, (N_S - 1)/2\} & N_S \text{ odd} \\ \{-(N_S - 2)/2, \dots, N_S/2\} & N_S \text{ even} \end{cases} \quad (12)$$

$$U = \{1, \dots, N_U\}. \quad (13)$$

and N_U is the length of the processed signal u and N_S is the length of the structuring element s .

In the case of the proposed method, the structuring element s_{50} contains only ones and is 50 ms long. This means, that the dilation operation (10) is in each step reduced to calculating the maximum value of the signal $|u_\varepsilon|$ using the samples that correspond to the ones in the structuring element in its current position. The structuring element is then moved by one sample and the maximum value of the corresponding part of the signal $|u_\varepsilon|$ is calculated. This is repeated N_U -times. After performing the dilation operation, the resulting signal is processed using the erosion operation (11). The same structuring element is used, only this time, the minimum values are calculated in each step. A more detailed description of this implementation of the closing operation can be found in [3].

A disturbance is detected when the signal after the closing operation u_{MORPH} exceeds the threshold level $Morph_THR$.

2.3. Classification

The classification of the detected disturbance is based on typical parameters of power quality events [7].

Disturbance is marked as a waveform distortion when it has a steady-state character, *i.e.*, when its duration is longer than 50 ms. This threshold is given by the length of the structuring element used in (8). The duration of the waveform distortions is determined using the time instants when the signal u_{MORPH} crosses the $Morph_THR$ threshold level. The magnitude of waveform distortions is determined as the maximum value of the signal u_{MORPH} during the disturbance.

Disturbances shorter than 50 ms are marked as transients. However, in this case, the signal with disturbances $|u_\varepsilon|$ has to be processed once again using the closing operation. This time, the structuring element (s_4) is only 4 ms long. Due to the long structuring element employed in (8) multiple transients that are close to each other could appear as a single disturbance in the signal u_{MORPH} . The shorter structuring element is used to obtain the signal u_{Mir} in which individual transients can be detected

$$u_{Mtr} = |u_\varepsilon| \bullet s_4. \quad (14)$$

Individual transients are detected by thresholding the signal u_{Mtr} with the same threshold level $Morph_THR$ as in the disturbance detection stage. The duration of the transients is determined using the time instants when the signal u_{Mtr} crosses this threshold level. The magnitude of transients is determined as the maximum value of the signal u_{Mtr} during the disturbance.

3. SIMULATION RESULTS

The proposed algorithm was implemented in Matlab and its performance was compared with the previously published method which uses a digital high-pass filter instead of sine-fitting [3]. To compare the two algorithms, a signal with a simulated transient was used. The signal is similar to the one used in [1] for testing of transient detection algorithms. The test signal is

$$u(t) = u_F(t) + u_{tr}(t). \quad (15)$$

where u_F is the fundamental with a frequency of 50 Hz and RMS value equal to 1 pu. The test signal is 10 cycles long. The transient, given by the component u_{tr} , is 2 cycles long and starts at the beginning of the 5th cycle

$$u_{tr}(t) = 0.1 \sqrt{2} \cos(2\pi 370 t) - 0.0522 \sqrt{2} \cos(2\pi 410 t). \quad (16)$$

Fig. 2 shows the test signal containing the simulated transient.

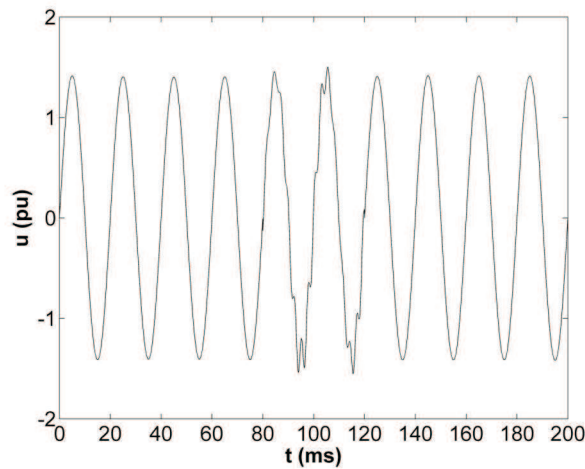


Fig. 2. Test signal used in simulations.

In Fig. 3, the transient components extracted using an IIR high-pass filter (Fig. 3b) and using the sine-fitting algorithm (Fig. 3c) are shown. Also shown in Fig. 3b and 3c are the differences between the extracted component u_e and the original transient u_{tr} . The cut-off frequency of the filter was 100 Hz and its attenuation in the stop band is 80 dB (for more details see [3]). From Fig. 3 it can be seen that the sine-fitting algorithm extracts the transient component more accurately. In case of the signal u_e extracted by the digital filter (Fig. 3b), there is a clearly visible distortion and overall phase-shift caused by the filter's non-linear phase response. However, the sine-fitting algorithm (mainly due to its iterative nature) is slower than filtering (in Matlab, it is approximately 5 times slower).

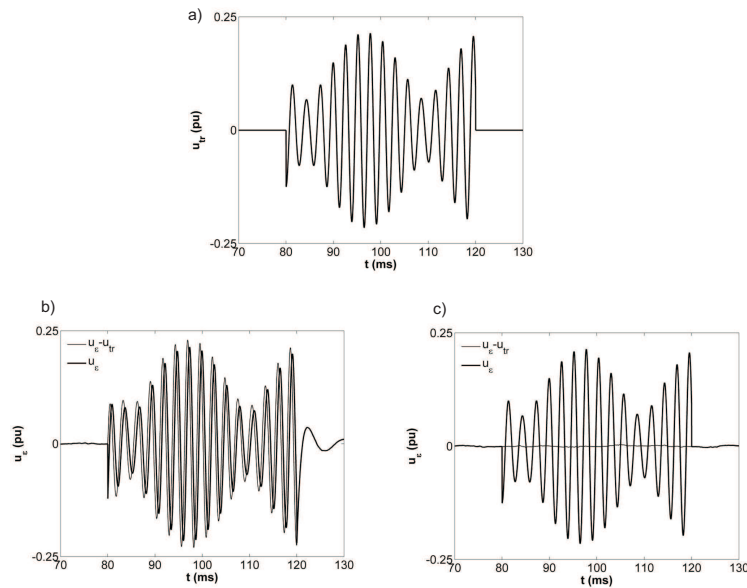


Fig. 3. Original simulated transient component (a) and the component extracted from the signal using b) digital filtering and c) sine-fitting.

4. EXPERIMENTAL RESULTS

In order to gather real single-phase power quality disturbances from the power network, a PC-based measuring setup was assembled (Fig. 4). The measuring setup contains a voltage transducer LEM CV 3-500 and data acquisition board (DAQ) NI USB-9215 (in Fig. 5 and 8 the transducer and the DAQ are included in the Sensor box). The nominal input RMS range of the transducer is 350 V and its frequency range is from DC up to 300 kHz. The sampling rate of the DAQ was set to 50 kS/s. The measured waveform was divided into data frames 10 cycles long to which the proposed algorithm was applied.

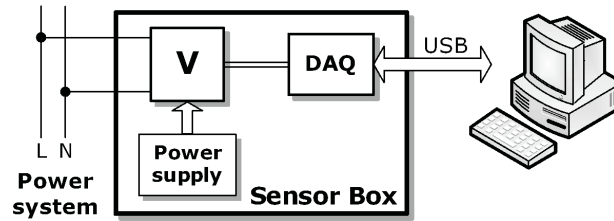


Fig. 4. Block diagram of the measuring setup implementing the proposed method.

The performance of the proposed method and its implementation in the measuring setup was compared with two commercial power quality analyzers: Fluke 434 and Chauvin Arnoux C.A 8334B. The Fluke 434 analyzer has an input range of 500 V, frequency bandwidth 100 kHz and sampling rate 200 kS/s per channel. The C.A 8334B has a voltage range of 480 V and sampling rate 12.8 kS/s per channel.

4.1. Measurement of disturbances in the power system

In the first measurement, the measuring setup with the proposed method and the two considered commercial power quality analyzers were connected to a single phase 230V/50Hz power system (see Fig. 5).

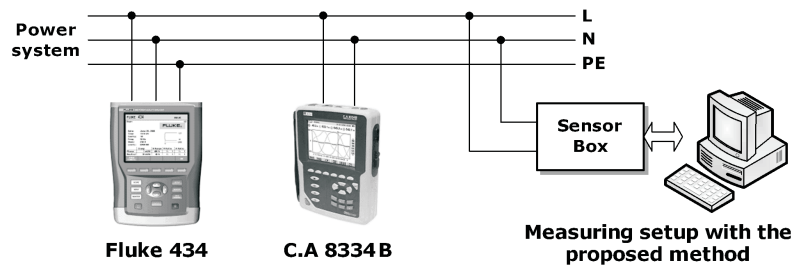


Fig. 5. Measuring setup for measuring of power quality disturbances in the power system.

Fig. 6 shows an example of one transient measured using the three considered instruments.

In Fig. 7, the processing of this transient using the proposed method is shown. One cycle of the voltage signal containing the transient together with the fundamental u_F estimated using the four-parameter sine-fitting algorithm is shown in Fig. 7a. In Fig. 7b the calculated transient component u_ε is shown. Figure 7c depicts the signals used to detect and classify the disturbance.

The magnitude of the disturbance measured by the proposed method was 0.59 pu and its duration was 1.9 ms. The magnitude measured by the C.A 8334B analyzer was 123.7 V (0.54 pu). The Fluke 434 analyzer does not extract any information (neither magnitude nor duration) about transients.

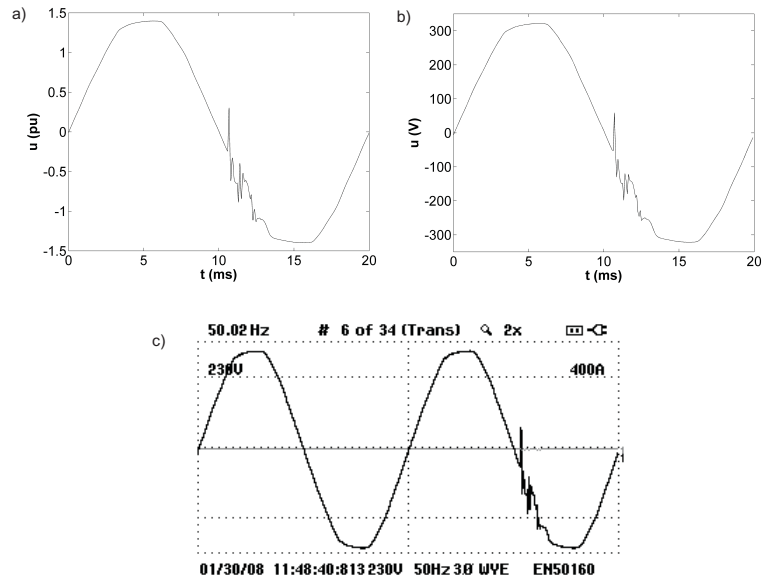


Fig. 6. An example of one transient measured using a) measuring setup with the proposed method; b) power quality analyzer Chauvin Arnoux C.A 8334B and c) power quality analyzer Fluke 434.

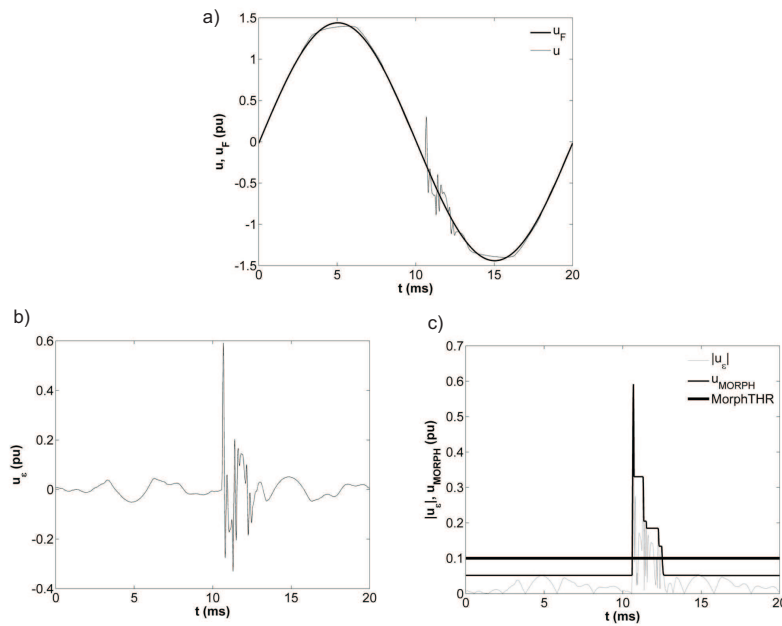


Fig. 7. Example of a measured transient a) voltage waveform with the fundamental; b) the transient component extracted using sine-fitting; c) signals used in disturbance detection.

4.2. Measurement of transients generated by a power source

In order to compare the detection capabilities of the proposed method with the two commercial power quality analyzers, the measuring set-up depicted in Fig. 8 was assembled.

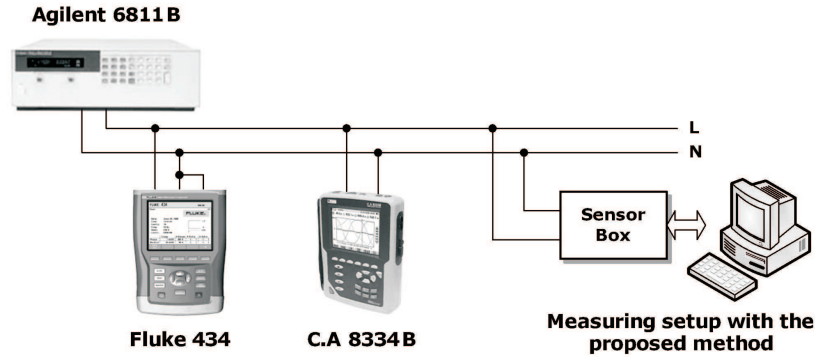


Fig. 8. Measuring setup for measuring of power quality disturbances generated by the power source.

In this setup, the power signal was generated by the Agilent 6811B Power Source. The power signal contained in every 10^{th} period one transient with specified parameters. Two types of transients were generated: i) impulsive transients (similar to the ones that originate from lightning strikes) and ii) oscillatory transients (which are caused in power systems e.g. by capacitor switching).

The impulsive transients were generated using

$$u_{TR}(t) = V_0 \left(e^{-t/\tau_b} - e^{-t/\tau_a} \right). \quad (17)$$

from [1] where $\tau_a = 71 \mu\text{s}$ and $\tau_b = 0.2 \mu\text{s}$. The value of V_0 was adjusted to obtain transients with the desired peak values.

The oscillatory transients were generated using

$$u_{TR}(t) = A_{TR} e^{-t/\tau} \cos(2\pi f_{TR} t). \quad (18)$$

from [1] where $\tau = 1 \text{ ms}$, $f_{TR} = 920 \text{ Hz}$. Due to the power source's limitations, it was not possible to generate transients with higher frequencies because the bandwidth of the employed power supply is 1 kHz. To cover at least the frequency range of low frequency oscillatory, an instrument with bandwidth of 5 kHz [7] would be required.

The detection thresholds of all instruments were set to approximately the same level. The threshold *Morph_THR* of the proposed method was set to 0.1 pu; the threshold of the Fluke 434 was set to 23 V and the detection threshold of the C.A 8334B was set to 10%. The analyzers Fluke 434 and C.A 8334B can only store 40 and 50 transients at a time, respectively, which limited the time of continuous measurement. All three instruments were set to an approximately 8 second long measurement. At

the end of the measurement interval, the success rate of detection of transients that occurred during this interval was evaluated.

Table 1 shows the percentage of impulsive transients detected by the instruments. Transients with peak values from $V_{PP} = 0.1$ up to 1.3 pu and in 3 different positions within the power signal's period ($\phi = 0^\circ, 30^\circ$ and 90°) were generated. Blank fields in the table represent configurations that the employed power source is not able to generate.

Table 1. Results of detection of impulsive transients using the considered power quality analyzers.

V_{PP} (pu)	$\phi = 0^\circ$			$\phi = 30^\circ$			$\phi = 90^\circ$		
	Proposed method	Fluke 434	C.A 8334B	Proposed method	Fluke 434	C.A 8334B	Proposed method	Fluke 434	C.A 8334B
0.1	100 %	12.5 %	0 %	100 %	0 %	0 %	100 %	0 %	0 %
0.2	100 %	100 %	83.3 %	100 %	100 %	81 %	100 %	67.5 %	81 %
0.3	100 %	100 %	81 %	100 %	100 %	81 %	100 %	100 %	81 %
0.4	100 %	100 %	81 %	100 %	100 %	83.3 %			
0.5	100 %	100 %	85.7 %	100 %	100 %	81 %			
0.75	100 %	100 %	83.3 %						
1.0	100 %	100 %	92.9 %						
1.3	100 %	100 %	81 %						

The proposed method was able to detect all transients. The Fluke 434 had problems detecting transients with the smallest magnitudes, however these problems may have been caused by the threshold setting (the disturbances with 0.1 pu have the same amplitude as the threshold level). The C.A 8334B had more problems detecting disturbances.

Table 2. Results of detection of oscillatory transients using the considered power quality analyzers.

A_{TR} (pu)	$\phi = 0^\circ$			$\phi = 90^\circ$			$\phi = 180^\circ$		
	Proposed method	Fluke 434	C.A 8334B	Proposed method	Fluke 434	C.A 8334B	Proposed method	Fluke 434	C.A 8334B
0.1	100 %	10 %	0 %	100 %	0 %	0 %	100 %	2.5 %	0 %
0.2	100 %	100 %	83.3 %	100 %	75 %	81 %	100 %	100 %	81 %
0.3	100 %	100 %	83.3 %	100 %	100 %	81 %	100 %	100 %	83.3 %
0.5	100 %	100 %	81 %				100 %	100 %	81 %
0.75	100 %	100 %	83.3 %				100 %	100 %	83.3 %
1.0	100 %	100 %	81 %				100 %	100 %	81 %
1.25	100 %	100 %	83.3 %						

Some can be attributed to the narrow frequency band. However, this does not explain all missed transients (especially the ones with greater magnitude).

Similar results were obtained in case of oscillatory transients as shown in Table 2. Again, the proposed method detected all transients, the Fluke 434 analyzer had problems with the smallest magnitudes and the C.A 8334B had a success rate just over 80% at best.

4.3. Measurement of waveform distortions generated by the power source

With the same measurement setup, the Agilent 6811B Power Source was configured to generate waveform distortions. In order to test the capability of the considered instruments to detect the disturbance and to determine its parameters (duration, magnitude), the generated signal was composed of 7 periods of a voltage signal without distortion and approximately 3 periods (59.96 ms) with added harmonic distortion. Due to the limitations of the power source in the arbitrary waveform mode, it is only possible to generate repeating patterns with 10 periods which limits the possible lengths of signal with and without distortion. The total harmonic distortion (THD) of the signal during the distortion was set to values from 1% to 15%. The distortion contained harmonics up to the 20th (the bandwidth of the power source is 1 kHz) and the phase of each higher harmonic was random.

The threshold *Morph_THR* of the proposed method was set to 0.065 pu. With this setting, the proposed method was able to detect all waveform distortions with THD greater than 3%. Figure 9 shows an example of a waveform distortion detected by the measuring setup with the proposed method. The THD during the distortion was 7.5%. The proposed algorithm determined the duration of the waveform distortion to be 59.88 ms and its magnitude (determined as the maximum value of the $|u_{MORPH}|$) to be 0.161 pu. The signals calculated in the course of detection and classification cannot be directly used to calculate the THD during the disturbance and some other methods would have to be employed (*e.g.*, multiharmonic sine-fitting [8]).

The Fluke 434 and C.A 8334B analyzers use values of total harmonic distortion calculated according to the IEC 61000-4-7 standard [9] to detect harmonic waveform distortions. Fluke 434 uses the group total harmonic distortion THDG [9, eq. 5]. C.A 8334B uses the total harmonic distortion THD [9, eq. 4]; however it uses a window 4 periods long [10] instead of 10 periods as required by the standard [9]. Because of the employed algorithms, neither of the analyzers was able to indicate the correct THD level of the disturbance which resulted in not being able to detect all generated waveform distortions. For example, when generating harmonic distortion with THD = 15%, Fluke 434 was showing THDG = 8.1% and C.A 8334B was showing THD between 0% and 11%. The IEC 61000-4-7 algorithms give a correct result only when the disturbance is presented in the whole 10 period window. The IEC 61000-4-7 algorithms cannot

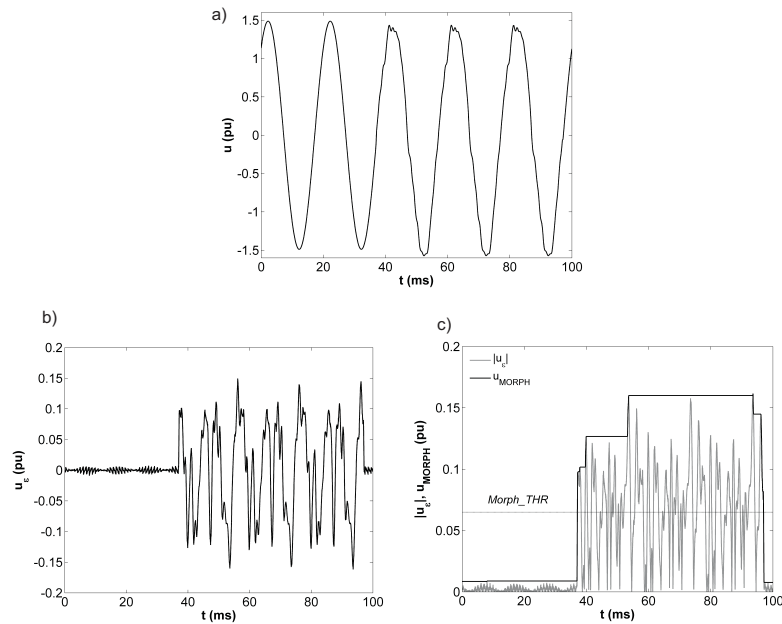


Fig. 9. Example of a waveform distortion generated by the power source a) voltage waveform containing the distortion; b) the waveform distortion extracted using sine-fitting; c) signals used in disturbance detection.

reliably detect distortions that are shorter than 10 periods even when their magnitude is significant and can cause problems to the equipment connected to the power system.

4.4. The proposed method and voltage fluctuations

Voltage fluctuations (which can be the origin of flicker [11]) are common in power systems. Although the proposed method does not include detection of voltage fluctuations it is important to test its behaviour (namely the behaviour of the 4-parameter sine-fitting algorithm) under these conditions.

In this measurement, the Agilent 6811B was programmed to generate a sine signal that included voltage fluctuation with $f = 5$ Hz and depth of modulation [11] $\Delta V/V = 10\%$. The 4-parameter sine-fitting algorithm was then applied to the signal acquired using the measuring setup. The algorithm was applied to segments of the measured voltage that were 10 000 samples long (10 periods of the power signal).

Figure 10a shows the estimated fundamental u_F and the measured voltage u . From this figure it can be seen that sine-fitting algorithm is able to work even when there is voltage fluctuation present in the voltage signal. The estimated amplitude of the fundamental is the average amplitude of the signal during the processed segment. Figure 10b shows the residuals after the sine-fitting. These residuals can be further

processed in order to obtain information about the fluctuation. Figure 11 shows the FFT spectrum of the residuals (for window length $N = 50\,000$ samples) which allows to determine e.g. the frequency of the voltage fluctuation.

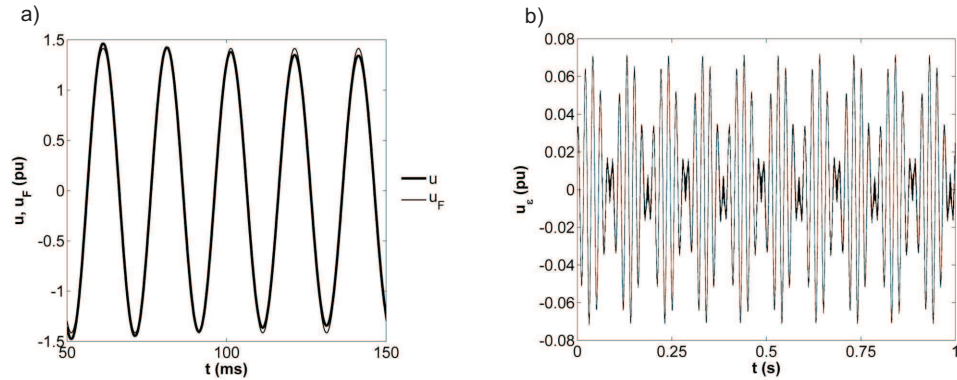


Fig. 10. Performance of the 4-parameter sine-fitting algorithm in the presence of voltage fluctuations: a) detail of the measured voltage u and estimated fundamental u_F ; b) the residuals after sine-fitting u_e .

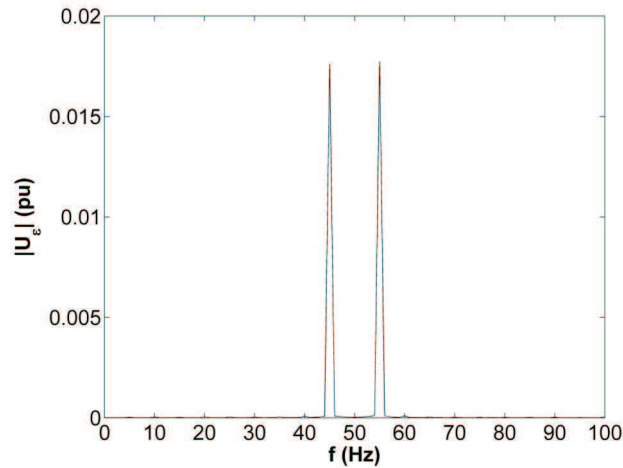


Fig. 11. FFT spectrum of the residuals shown in Fig. 10b.

5. CONCLUSIONS

A new method for detection and classification of transients and waveform distortions is presented in this paper. The method uses a modified version of the four-parameter sine-fitting algorithm and the morphology operation closing to extract and process the transient component of the voltage in the power system.

The proposed method was compared with a previously developed method based on a digital high-pass filter. The proposed method is slower but it is more accurate because it does not experience the problems with the non-linear phase response characteristic of IIR filters. As a by product, the sine-fitting algorithm returns the estimates of the instantaneous frequency and amplitude of the voltage's fundamental which can be used in further analysis of the power quality.

The performance of the proposed method was compared with two commercial power quality analyzers: Fluke 434 (which complies with the IEC 61000-4-30 Class B specification) and C.A 8334B. The three instruments were used for monitoring of a single-phase power system. During the monitoring they were able to detect all disturbances that occurred during the monitoring. However, due to the limited memory of the commercial power quality analyzers, the monitoring period was limited to approximately 2 hours (because of the number of disturbances that occur in the monitored power system). For a more detailed comparison of the performance, a power signal containing transients with different characteristics was generated using the Agilent 6811B Power Source. The performance of the proposed method was the same or better as the performance of the Fluke 434 analyzer.

Even though the presented measurements do not represent a full test of compliance with power quality standards they show that the proposed method is suitable for reliable and on-line detection of the considered power quality disturbances. In case of waveform distortions, the proposed method offers higher time resolution than the methods based on the IEC 61000-4-7 standard.

ACKNOWLEDGEMENT

Work sponsored by the Portuguese national research project reference POSC/EEA-ESE/57708/2004 entitled "Fast and accurate power quality measurements using analog to digital converters and digital signal processing techniques".

REFERENCES

1. Bollen M. H. J., Gu I. Y. H.: *Signal Processing of Power Quality Disturbances*, John Wiley & Sons, 2006.
2. Santoso S., Powers E. J., Grady W.M., Hofmann P.: "Power quality assessment via wavelet transform analysis". *IEEE Trans. Power Del.*, vol. 11, no. 2, 1996, pp. 924–930.
3. Radil T., Ramos P. M., Janeiro F. M., Serra A. C.: "DSP Based Power Quality Analyzer for Detection and Classification of Disturbances in a Single-phase Power System". *Metrology & Measurement Systems*, vol. XIV, no. 4, 2007, pp. 483–494.
4. *IEEE Std 1057-1994, IEEE Standard for Digitizing Waveform Recorders*, The Institute of Electrical and Electronics Engineers, Inc., New York, 1995.
5. Renders H., Schoukens J., Vilain G.: "High-Accuracy Spectrum Analysis of Sampled Discrete Frequency Signals by Analytical Leakage Compensation". *IEEE Trans. Instr. Meas.*, vol. 33, no. 4, 1984, pp. 287 – 292.

6. Serra J.: *Image Analysis and Mathematical Morphology*, vol. 1. Academic Press, 1982.
7. *IEEE Std. 1159-1995, IEEE Recommended Practice for Monitoring Electric Power Quality*, The Institute of Electrical and electronics Engineers, Inc., New York, 1994.
8. Ramos P. M., da Silva M. F., Martins R. C., Serra A. M. C.: "Simulation and experimental results of multiharmonic least-squares fitting algorithms applied to periodic signals". *IEEE Trans. Instrum. Meas.*, vol. 55, no. 2, 2006, pp. 646–651.
9. IEC 61000-4-7 Electromagnetic compatibility (EMC) – Part 4-7: Testing and measurement techniques (General guide on harmonics and interharmonics measurement and instrumentation, for power supply systems and equipment connected thereto), 2nd edition, 2002.
10. C.A 8334B User's Manual, Chauvin Arnoux, 2nd edition, <http://www.chauvin-arnoux.com>, 2007.
11. IEC 61000-4-15 Electromagnetic compatibility (EMC) – Part 4-15: Testing and measurement techniques, (Flickermeter – functional and design specifications), edition 1.1, 2003.